THE IMPACT OF SLIP ON NANOCHANNEL FRICTION FACTOR

Filippos Sofos[1], Theodoros E. Karakasidis and Antonios Liakopoulos

Hydromechanics and Environmental Engineering Laboratory, Department of Civil Engineering, University ofp Thessaly, Volos 38334, Greece
[1]fsofos@uth.gr

Abstract. *We present slip length calculations based on data compiled from Molecular Dynamics simulations so as to estimate the Darcy-Weisbach friction factor, f, in nanochannel flows. We present a correlation scheme that modifies the macroscopic Poiseuille flow relation* $f = 96/\mathrm{Re}$ *when we take into account the slip length at the wall, which is present at the nanoscale. The slip length is affected by channel parameters significant at the nanoscale, although insignificant at the macroscale, such as wall wettability, wall roughness and stiffness, external force magnitude and temperature. Results indicate that larger slip lengths are observed at small channel widths and past an hydrophobic wall. Calculations show that the friction factor (or, equivalently, the energy loss), is significantly reduced as the slip length increases.*

Keywords: Molecular Dynamics, Nanoflows, Slip length, Darcy friction factor, Energy Loss.

1 INTRODUCTION

Molecular Dynamics (MD) can be employed to perform simulations of nano-scale systems in high detail. It has been successfully used to study the behavior of water cleaning and purification [1-2], crystal formation [3] and chemical reactions [4]. However, MD is computationally intensive since it involves calculations at the atomic level, with systems comprising hundreds of thousands of molecules to fit engineering applications. Nevertheless there are cases where, no matter how close to the nanoscale we are, it is possible to employ relations from the continuum theory after some adjustments [5-6]. Another popular method is the hybrid MD-continuum method, which involves multiscale caclulations at various scales [7-8].

Most atomistic methods agree that the breakdown of the no-slip assumption, which is valid at the macroscale, takes place at the nanoscale. The presence of roughness in nanochannel walls is one of the main parameters that control the value of the slip length. It has been found [9] that, under specific rough-wall characteristics, significant reductions in the frictional pressure drop and greater effective fluid slip at the walls can be achieved relative to the classical smooth channel Stokes flow. Priezjev [10] reported that slip length reduces by periodic and random surface roughness, compared to atomically smooth rigid walls, while, it has been shown that fluid atom trapping inside the grooves [11] of a rough wall could also affect slip length values.

The effect of surface characteristics on flows also involves wall wettability parameter. Wall hydrophobicity has been found to increase slip, while hydrophilic walls may lead to sticking phenomena [12]. Terms like super- or ultra- hydrophobic surfaces have been incorporated in order to describe hydrophobic surfaces (and rough at the same time) where the contact angle, θ, is greater than 150^o. The experimental work of Ou et al. [13] reveals drag reduction in ultrahydrophobic surfaces. However, there are cases where results are contradicting, for example, in Yang [14], it is noted that fluid molecules flowing over a rough surface (both hydrophobic and hydrophilic, for various geometrical characteristics of wall roughness) lose more tangential momentum than the smooth surfaces, resulting in the reduction of slip length.

From a different point of view, when considering polar liquid flow, the amount of slip seems to depend on the polarity of the liquid molecules [15], while, the molecular structure of the liquid is also a factor that affects slip length value [16]. Slip is also produced by wall stiffness (rigid or "loose" wall) [17].

In this work, Molecular Dynamics simulations are applied in order to investigate liquid flows in nanochannels, quantify the slip length at the wall and estimate the respective energy losses through the friction factor calculation. Our results reveal that slip exists at the nanoscale and its value is significantly affected by geometrical characteristics of the surface, wall/fluid interactions, forces that drive the flow and parameters that constitute our simulation model. Furthermore, the friction factor, *f*, in Poiseuille flow, although a macroscale quantity, is affected by fluid ordering at the nanoscale and deviates from the classical value of $f = 96/\mathrm{Re}$, where, Re, the Reynolds number.

2 THEORETICAL CALCULATIONS

Let's assume that the continuum assumption is valid, the fluid is Newtonian, all assumptions listed on page 165 of [18] are valid, and the shear viscosity $\mu = \text{const.}$

We simplify Navier-Stokes (NS) equations for Poiseuille flow with slip and obtain

$$\frac{\mathrm{d}}{\mathrm{d}y}\left(\mu\frac{\mathrm{d}u}{\mathrm{d}y}\right) = G \quad \underset{\mu=\text{const.}}{\Rightarrow} \quad \frac{\mathrm{d}^2u}{\mathrm{d}y^2} = \frac{G}{\mu} \tag{1}$$

with B.C.: $u\left(y = \mathrm{h} + \mathrm{b}^*\right) = 0$ and $u\left(y = -\mathrm{h} - \mathrm{b}^*\right) = 0$, where b^* is the slip length measured as the length of the velocity profile that "enters" the wall region (see Fig. 1(a)).
Integrating twice and incorporating the B.C.s we obtain

$$u = \frac{G}{2\mu}\left[y^2 - \left(\mathrm{h} + \mathrm{b}^*\right)^2\right] \tag{2}$$

The average velocity is given from

$$\overline{\mathrm{V}} = \frac{\int_{-\mathrm{h}}^{\mathrm{h}} u\mathrm{d}y}{2\mathrm{h}} = \frac{G}{2\mu}\left[\frac{\mathrm{h}^2}{3} - \left(\mathrm{h} + \mathrm{b}^*\right)^2\right] \tag{3}$$

The Darcy-Weisbach friction factor, in terms of the shear stress at the wall, τ_w, is expressed as

$$f = \frac{8\tau_w}{\rho\overline{\mathrm{V}}^2} \tag{4}$$

After some algebra we find that

$$f = \left[\frac{96}{\mathrm{Re}_{\mathrm{D_h}}}\right]\left[\frac{2}{3\left(1 + \dfrac{\mathrm{b}^*}{\mathrm{h}}\right)^2 - 1}\right] \tag{5}$$

It is easily proved by geometric arguments that

$$\mathrm{b} = \mathrm{b}^* + \frac{\left(\mathrm{b}^*\right)^2}{2\mathrm{h}} \quad \Leftrightarrow \quad \frac{\mathrm{b}}{\mathrm{h}} = \frac{\mathrm{b}^*}{\mathrm{h}} + \frac{1}{2}\left(\frac{\mathrm{b}^*}{\mathrm{h}}\right)^2 \tag{6}$$

Plugging Eq. (6) in Eq. (5) we obtain

$$\mathrm{f} = \left[\frac{96}{\mathrm{Re}_{\mathrm{D_h}}}\right]\left[\frac{1}{1 + 3\dfrac{\mathrm{b}}{\mathrm{h}}}\right] \tag{7}$$

or

$$\mathrm{f} = \left[\frac{96}{\mathrm{Re}_{\mathrm{D_h}}}\right]\left[\frac{1}{1 + 6\dfrac{\mathrm{b}}{\mathrm{H}}}\right] \tag{8}$$

where $\mathrm{H} = 2\mathrm{h}$ and b is the standard definition of slip length (based on the tangent of the velocity profile at the macroscopically flat wall, see Fig. 1(a)). A similar form of Eq. 8 is presented in [19].

We define as M_f the modification factor derived in Eq. (8)

$$\mathrm{M_f} = \left[\frac{1}{1+6\frac{\mathrm{b}}{\mathrm{H}}} \right] \tag{9}$$

and write

$$\mathrm{f} = \left[\frac{96}{\mathrm{Re_{D_h}}} \right] M_f \tag{10}$$

We remind the reader that in the continuum theory of Poiseuille flow with μ=const. and the no-slip condition enforced at the walls, M_f=1.

The Reynolds number is defined here as

$$\mathrm{Re} = \frac{\mathrm{vD_h}}{\nu} \tag{11}$$

or

$$\mathrm{Re} = \frac{\mathrm{vD_h}}{\mu/\rho} \tag{12}$$

where ν is the kinematic viscosity, μ the shear viscosity and $\mathrm{D_h}$ is the hydraulic diameter.

3 MOLECULAR DYNAMICS METHOD

Liquid monoatomic flow is simulated in channels with flat and rough walls (Figs. 1(a-b), respectively). Flow is considered equivalent to Poiseuille flow, where a monoatomic liquid flows between two parallel, infinite plates. The system is periodic along the x-, and z-directions, while, in y-direction, $H=2h$ is the wall separation (channel height). Wall separation for the flat-wall channel is investigated for H=0.9-6.3nm, while groove height and length for the rough-wall channels are investigated for a range of values, $0.6 \le h_d \le 1.96nm$ and $0.3 \le h_l \le 1.8nm$, respectively.

The Molecular Dynamics method is based on the calculation of interactions between wall and fluid particles with the 12-6 Lennard-Jones potential $u^{LJ}(r_{ij}) = 4\varepsilon((\sigma/r_{ij})^{12} - (\sigma/r_{ij})^{6})$, with parameters for length, σ = 0.3405 nm and energy, ε/k_B = 119.8 K, and constant fluid density ρ=1078 Kg/m^3. Flow is induced due to the application of an external force F_{ext} =0.036 pN to all fluid atoms, which acts as an analog to the application of pressure difference to induce the flow in macroscopic systems. The system is simulated for various wall/fluid interaction energy ratios $\varepsilon_w/\varepsilon_f$ (w: wall and f: fluid), which have been found to be analogous to surface wettability, i.e., $\varepsilon_w/\varepsilon_f$ < 0.5 for an hydrophobic wall, while $\varepsilon_w/\varepsilon_f$ >0.5 for an hydrophilic wall.

Wall atoms are bound on fcc sites and remain fixed to their original positions due to the effect of an elastic spring force $\mathbf{F} = -K(\mathbf{r}(t) - \mathbf{r}_{eq})$, where $\mathbf{r}(t)$ is the vector position of a wall atom at time t, $\mathbf{r}_{eq}$ is its initial lattice position vector and K the wall spring constant. Fluid temperature is kept constant to T=120K, through the application of two independent Nosé-Hoover thermostats at each thermal wall. The simulation step is $\Delta t=10^{-2}$ps. Simulation begins with fluid atoms given appropriate initial velocities in order to reach the desired temperature. The system reaches equilibrium after an equilibrium run of $2\text{x}10^6$ time steps. Then, a number of NEMD simulations for each channel type are performed, each with duration of $5\text{x}10^5$ time steps.

4 RESULTS AND DISCUSSION

4.1 Velocity profiles

In order to compute the velocity profile, the channel is divided into n=40 bins along the y-direction, each one of volume L_x x L_z x (H/n). To extract the velocity profiles for a flat-wall channel, average velocity is computed at

each bin for each time step and all these values are averaged. For a rough-wall channel, velocity profiles across roughness protrusions and cavities are calculated and, finally, averaged. Results are depicted in Figs. 2(a-e).

Figure 2(a) presents the effect of the channel width, under the same flow conditions. There is a clear increase in velocity values across the channel as system dimensions increase. As, also, expected, an increase in the magnitude of the external force induces additive energy to the system and velocity values increase (Fig. 2(b)). The range of external force values investigated in this work varies from the minimum value for the flow to begin to the maximum value for not inducing excessive shear stresses and non-linearity. As far as wall wettability is concerned (Fig. 2(c)), we observe that a highly hydrophobic wall ($\varepsilon_w/\varepsilon_f = 0.2$) leads in increased velocity values across the channel, compared to values obtained from flow between highly hydrophobic walls ($\varepsilon_w/\varepsilon_f = 5.0$).

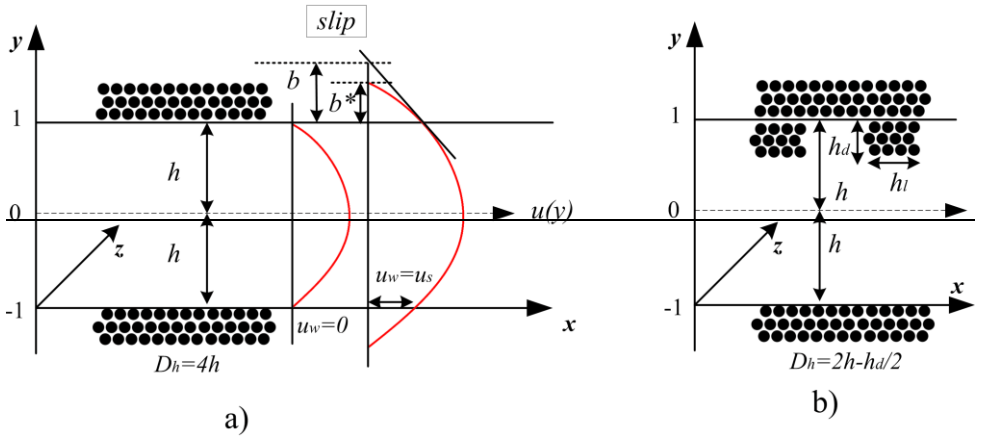

Figure 1. a) Atomistic model of Poiseuille flow at the nanoscale. Velocity profiles with slip and no-slip are shown. b) Atomistic model of flow in rough-wall nanochannels, where h_l is the length and h_d is the height of roughness rectangular protrusions. D_h is the hydraulic diameter.

Velocity profiles obtained from rough-wall channel flow, seem not to be significantly affected by a change in the length, h_l, of the protruding rectangular elements that constitute the rough wall (Fig. 2(d)), although a shift to the left is observed in all profiles (compared to a flat-wall velocity profile), as the right side is the rough one. On the contrary, in Fig. 2(e), where roughness depth, h_d, increases and the protruding elements develop towards the channel midplane, the flows seems to slow down, velocity values decrease significantly and the profiles present inhomogeneity, as they are divided by the protrusions in two almost distinct parabola. Finally, velocity profiles affected by the spring constant, K, variations for a rough-wall channel are shown Fig. 2(f). As K increases, walls become stiffer and there is a trend that velocity values slightly increase.

4.2 Slip Length

From velocity values presented in Section 4.1, we derive slip length at the wall $b = u_w \Big/ \left.\frac{du}{dy}\right|_w$ (based on the tangent of the velocity profile at the macroscopically flat wall, see Fig. 1(a)), for the respective simulation conditions. We observe that slip length is larger as the channel height decreases to the atomic scale (Fig. 3(a)). In Fig. 3(b), the external force that drives the flow has a small effect on slip, as, at least for the range examined in this work, it seems to decrease the slip length as F_{ext} magnitude increases. As expected from literature findings [12-13], an hydrophobic wall is the main parameter that can facilitate flows through slip length increase. Moreover, the hydrophilic wall leads to fluid atom stick in channel layers adjacent to the wall, as b values reveal in Fig. 3(c). Roughness length, h_l, is a rough-wall property that affects slip length (Fig. 3(d)). Greater slip length is achieved when this roughness parameter is small and this value is slightly decaying as h_l increases. When the roughness height, h_d, is increased, flow is blocked by the protrusions that enter the flow region and slip length obtains large values. The effect of the spring constant K on slip length is not monotonic, as we observe in Fig. 3(f). We obtain large slip both for small and large values of K, and a minimum for an intermediate K value. When wall atoms are not strongly fixed, atomic-scale roughness is created at the surface and this should be the reason why the fluid presents slip.

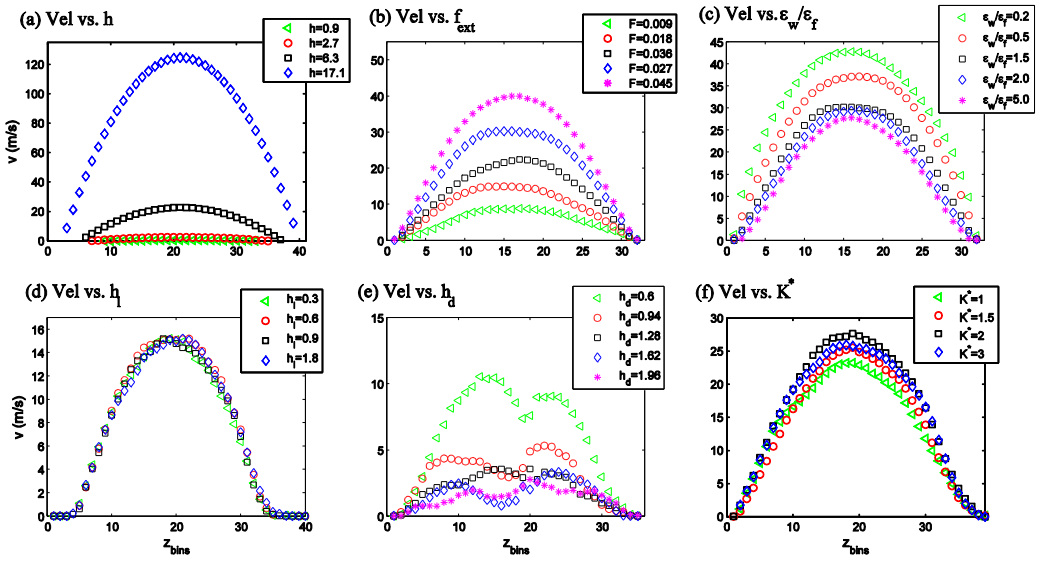

Figure 2. Effect of a) channel width (flat-wall channels, F_{ext}=0.018pN, K^*=1, $\varepsilon_w/\varepsilon_f$ =1.2), b) magnitude of the external force (flat-wall channels, H=6.3nm, K^*=1, $\varepsilon_w/\varepsilon_f$ =1), c) wall wettability ratio (flat-wall channels, H=6.3nm, K^*=1, F_{ext}=0.036pN), d) roughness length (rough-wall channels, K^*=1, $\varepsilon_w/\varepsilon_f$ =1, h_d =0.6nm), e) roughness height (rough-wall channels, K^*=1, $\varepsilon_w/\varepsilon_f$ =1, h_l =1.8nm, F_{ext}=0.018pN) and f) spring constant value (rough-wall channels, $\varepsilon_w/\varepsilon_f$ =1, h_l =1.8nm, h_d =0.6nm, F_{ext}=0.036pN) on velocity profiles.

4.3 Modification factor

The modification factor derived in Eq. (9) can be a means of estimating the degree of application of the continuum theory towards the atomistic scale. Having in mind that the slip length is one of the dominant features that characterize nanoflows, we calculate M_f and plot $f \times \mathrm{Re}$ values vs. Channel flow parameters in Fig. 4(a). When M_f=1, then $f \times \mathrm{Re} = 96$ and this limit is indicated with the dotted, black line. In this concluding diagram, we observe that parameters that affect flow at the nanoscale have a significant impact on friction factor values. We do not deviate from the continuum theory for channel heights above h≈6-7nm, while for channels of smaller height, the modification factor increases significantly. The magnitude of the external driving force could affect m_f in two ways; a small value leads to $f \times \mathrm{Re} > 96$, while larger values lead to $f \times \mathrm{Re} < 96$. Hydrophobic channel flows ($\varepsilon_w/\varepsilon_f$ < 0.5) need a modification factor $M_f < 1$ while, as the wall becomes more hydrophilic, m_f increases above one. For the remaining parameters, e.g., roughness length, roughness height and wall spring constant, we obtain $f \times \mathrm{Re} < 96$, and this is attributed to small re numbers in such nanochannel flows. An exception occurs when h_d=20%h, a case of large slip length, where $f \times \mathrm{Re} \approx 250$.

If we plot f vs. Re at the nanoscale, then we could expand the classical Moody's diagram to the left; to a low-Re values region. Figure 4(b) presents logarithmic values of f vs. Re for all flow cases investigated here. Dotted line indicates the continuum limit, f=96/Re. We observe that our data are well-organized on f=96/Re for all cases of channel height, external force, roughness length and spring constant values we investigated. We only deviate from the continuum limit when we vary wall wettability and roughness heights.

5 CONCLUSIONS

An investigation of internal flows exhibiting slip at the nanoscale has been performed and compared with a continuum theoretical flow model. The presence of slip length, b, is shown to have a significant effect on nanoscale Darcy-Weisbach friction factor, as a large slip length value decreases f. The dominant parameters in nanoflows that affect slip length are the hydrophobicity/hydrophilicity of the wall and wall roughness height,

which are not taken into account at the macroscale. We show that a modification factor, M_f, is employed at the nanoscale in order to incorporate nanoflow scale effects in the classical Poiseuille relation for planar geometry $f = 96/\mathrm{Re}$, which now becomes $f = (96/\mathrm{Re})M_f$. For flat channel walls the modification factor acts as a means of quantifying the limit of continuum theory, by incorporating slip length values coming from atomistic simulations. For more general wall morphology, results show that the basic form of the friction factor correlations breaks down only when wall protrusions are large enough to block the flow and walls are of increased hydrophilicity.

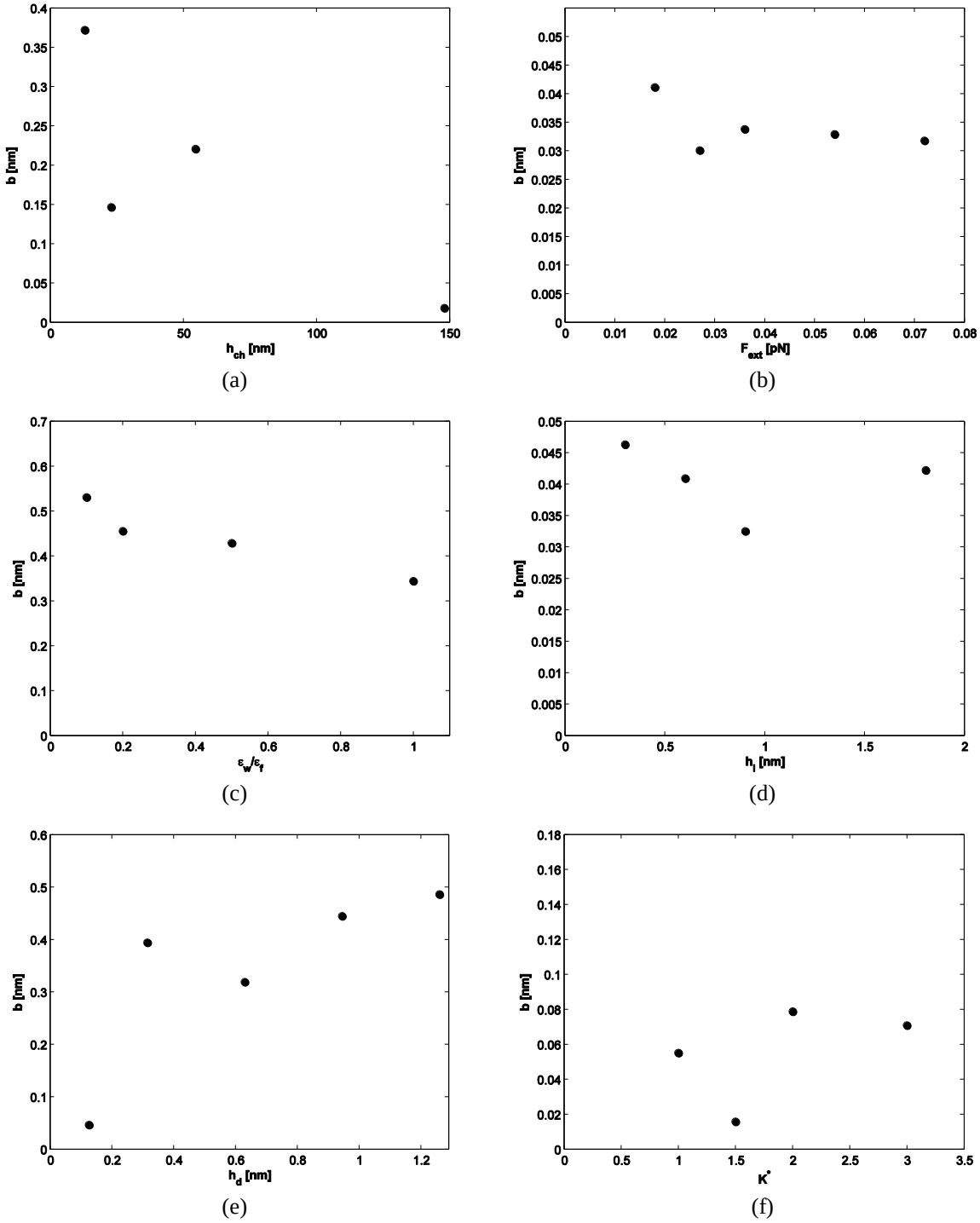

Figure 3. Slip length, *b*, vs. a) channel width, b) magnitude of the external force, c) wall wettability ratio, d) roughness length, e) roughness height and f) spring constant value. Simulation conditions are the same as the respective cases in Fig. 2.

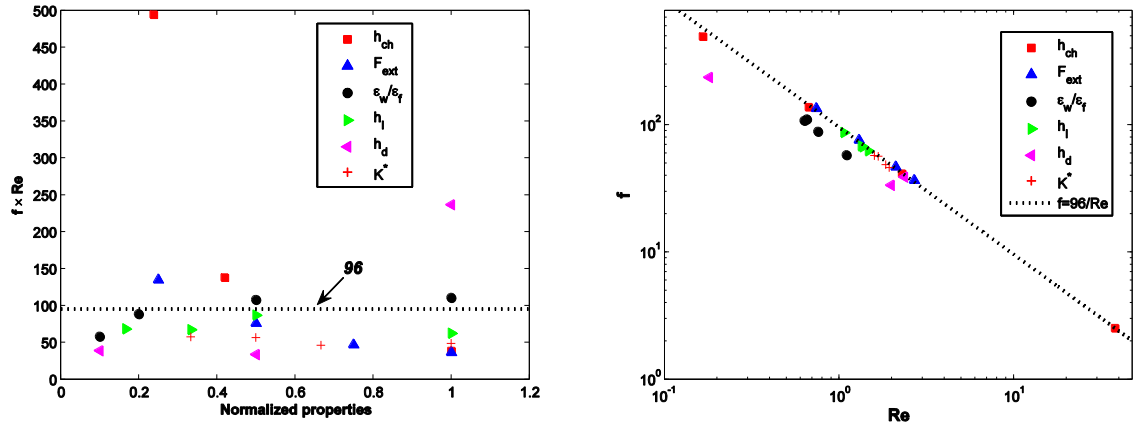

Figure 4. a) The modification factor (Eq. (9)) for various nano-flow conditions. Each parameter on the horizontal axis is normalized to its maximum value for presentation reasons and b) *f* vs. Re fully logarithmic diagram.

Acknowledgement: This project was implemented under the "ARISTEIA II" Action of the "OPERATIONAL PROGRAMME EDUCATION AND LIFELONG LEARNING" and is co-founded by the European Social Fund (ESF) and National Resources.

REFERENCES

[1] Humplik T., Lee J., O'Hern S.C., Fellman B.A., Baig M.A., Hassan S.F., Atieh M.A., Rahman F., Laoui T., Karnik R., and Wang E.N. (2011), "Nanostructured materials for water desalination," *Nanotechnology*, Vol. 22, p. 292001.

[2] Ritos K., Mattia D., Calabrò F., and Reese, J.M. (2014), "Flow enhancement in nanotubes of different materials and lengths," *The Journal of Chemical Physics*, Vol. 140, p. 014702.

[3] Parrinello, M. and Rahman, A. (1980) "Crystal structure and pair potentials: A molecular-dynamics study," *Physical Review Letters*, Vol. 45, pp. 1196-1198.

[4] Sheehan, M.E. and Sharratt, P.N. (1998), "Molecular dynamics methodology for the study of the solvent effects on a concentrated dielsalder reaction and the separation of the post-reaction mixture," *Computers & Chemical Engineering*, Vol. 22, pp. S27-S33.

[5] Sofos, F., Karakasidis, T.E., and Liakopoulos, A. (2015), "Fluid structure and system dynamics in nanodevices for water desalination," *Desalination and Water Treatment* (accepted).

[6] Giannakopoulos, A.E., Sofos, F., Karakasidis, T.E., and Liakopoulos, A. (2014), "A quasi-continuum multi-scale theory for self-diffusion and fluid ordering in nanochannel flows," *Microfluidics & Nanofluidics*, Vol. 17, pp. 1011-1023.

[7] Kalweit M., and Drikakis, D. (2008), "Coupling strategies for hybrid molecular-continuum simulation methods," *Proceedings of the Institution of Mechanical Engineers, Part C*: *Journal of Mechanical Engineering Science*, Vol. 222, pp. 797-806.

[8] Asproulis N. and Drikakis D. (2013), "An Artificial Neural Network based Multiscale Method for Hybrid Atomistic-Continuum Simulations," *Microfluidics & Nanofluidics*, Vol. 15, 559-574.

[9] Davies, J., Maynes, D., Webb, B.W., and Woolford, B. (2006), "Laminar flow in a microchannel with superhydrophobic walls exhibiting transverse ribs," *Physics of Fluids*, Vol. 18, p. 087110.

[10] Priezjev, N.V. (2007) "Effect of surface roughness on rate-dependent slip in simple fluids," *The Journal of Chemical Physics*, Vol. 127, 144708.

[11] Sofos, F.D., Karakasidis, T.E., and Liakopoulos, A. (2009), "Effects of wall roughness on flow in nanochannels," *Physical Review E*, Vol. 79, p. 026305.

[12] Baudry J. and Charlaix E. (2001) "Experimental Evidence for a Large Slip Effect at a Nonwetting Fluid - Solid Interface," *Langmuir*, Vol. 4, pp. 5232–5236.

[13] Ou J., Perot B., and Rothstein, J.P. (2004) "Laminar drag reduction in microchannels using ultrahydrophobic surfaces," *Physics of Fluids*, Vol. 16, pp. 4635–4643.

[14] Yang S.C. (2006) "Effects of surface roughness and interface wettability on nanoscale flow in a nanochannel," *Microfluidics & Nanofluidics*, Vol. 2, pp. 501–511.

[15] Ulmanella U. and Ho, C.-M. (2008) "Molecular effects on boundary condition in micro/nanoliquid flows," *Physics of Fluids*, Vol. 20, p. 101512.

[16] Vadakkepatt, A., Dong, Y., Lichter, S., and Martini, A. (2011) "Effect of molecular structure on liquid slip," *Physical Review E*, Vol. 84, p. 066311.

[17] Asproulis N. and Drikakis D. (2010), "Boundary slip dependency on surface stiffness," *Physical Review E*, Vol. 81, p. 061503.

[18] Liakopoulos A. "Fluid Mechanics", Tziolas Publications (in greek), 2010. ISBN 978-960-418-324-1

[19] Enright, R., Eason, C., Dalton, T., Hodes, M., Salamon, T., Kolodner, P., Krupenkin, T. (2006) "Friction Factors and Nusselt Numbers in Microchannels With Superhydrophobic Walls," *Proceeding of the ASME 4th International Conference on Nanochannels, Microchannels, and Minichannels*, Limerick, Ireland, 2006, No. 96134, pp. 1-8.